2nd International Conference on
CIVIL ENGINEERING, ARCHITECTURE & URBAN PLANNING ELITES
15th Nov.2016 London - United Kingdom
دومین کنفرانس بین المللی
نخبگان عمران، معماری و شهرسازی
لندن - انگلستان ۲۵ آبان ماه ۱۳۹۵

Optimal forms of two-pin arches

Asal Pournaghshband
PhD graduate Warwick University
A.Pournaghshband@wawick.ac.uk

Abstract
A comprehensive review of the response of two-pin arches including catenary, parabolic and circular form to loading is presented. The effects of form on the arch structural response for static loading and span-to-height ratios (*L:h*) ranging from 2 to 8 are presented using finite element solution provided by the *GSA* software. Results have shown that circular arches represent least optimal shape, exhibiting high combined stresses and bending moments, particularly for the *L:h* ratio of 2 (semi-circular arch). The optimum *L:h* ratio for a circular rib arch is between 4 and 6, but the stresses that develop in it are still higher than in parabolic or catenary arches. This is with regard to the pure arch behavior for $L{:}h \leq 5$. The minimum of the combined compressive stresses in parabolic and catenary arches are observed at *L:h* ratio between 2 and 4. The parabolic arch demonstrated lower structural action effects when the uniformly distributed load (*UDL*) is greater than the self-weight (*SW*). Overall, the findings demonstrate that the response of 2-pin arch forms to applied loading is critically dependent on the arch form and its shape governed by the *L:h* ratio.

Keywords: form; span-to-height; combined stress; bending moment; optimal

1. Introduction

One of the oldest forms of structures in the engineering field is arch structures. The use of arches started with the ancient Romans and continues to this day with different applications in many diverse fields (Ambrose and Tripeny, 2011). Proske and Pieter stated that the use of circular arches was remarkable during the 14th and 15th centuries in the shape of filled barrel stone arch. In the late 16th century, the arch building industry entered a new stage of development, when new spans exceeded using other arch forms, although circular arches were still being widely used (Proske and Pieter, 2009). The question of what shape of arch is preferable was not raised until 1675 (Heyman, 1998). It was when Hook stated an anagram in Latin translating "as hangs the flexible line, so but inverted will stand the rigid arch" (Heyman, 1998). This philosophy was put into practice by Antonio Gaudi (Tomlow et al, 1989). Gaudi was well known for his novel forms of vertical and inverted catenaries. Following, the stability of catenary arches subjected to self-weight only was examined at the University of Stuttgart by Tomlow et al. in 1989. There, it was shown that catenary arch is preferred in design when subjected to self-weight only which known as momentless arch.

In research into the impact of *L:h* ratio of two-dimensional parabolic, circular and catenary arches on buckling loads, Austin and Ross produced a comprehensive numerical study (Austin and Ross, 1976). In their assessments, the arches were assumed to be slender, and shear deformations was ignored. The authors illustrated that the critical horizontal reactions for the asymmetrical buckling modes were sensitive to changes in *L:h* ratios. Their findings concerned both two-pin and fixed arches under uniformly distributed load. They showed that, for *L:h* ratio between 2 and 5, parabolic arches could carry 10-48% higher buckling loads than circular forms, and 9-30% higher buckling loads than catenary arches. Hence, they concluded that parabolic arches were preferable to circular and catenary ones when buckling loads are evaluated. Moreover, it was seen that the buckling load of the arches is affected by the *L:h* ratios and the arch shape. Later Harvey and Smith defended semi-circular arches as sound and aesthetic forms, when they are subjected to surcharge due to ground fill exerting horizontal forces (Harvey and Smith, 1987). This case is an exception to general findings, including the results presented in this paper that confirm a circular arch form to be less efficient than parabolic or catenary shapes. Further, their method was based on the thrust line analysis that produces inaccurate results. The authors concluded that an ideal arch shape did not exist, and that an optimal arch form may be found for specific loading configurations. Fairfield and Ponniah used a series of timber model tests to study the behavior of backfilled arch bridges (Fairfield and Ponniah, 1994). In their experimental investigation most of the tests carried out involved a parametric study of circular buried arch bridges, considering various fill depths. The fill depth at the crown and the load location were considered as variables. They found the collapse load, at the *L:h* ratio of 2 (semi-circular form), to be 20– 45% of the collapse load at the *L:h* ratio of 4. Thus, the circular arch was more efficient at higher *L:h* ratio, as far as the collapse load's tolerance was concerned. Unfortunately, their assessment was limited to arches with *L:h* ratios of 2 and 4, respectively. Following, Bensalem et al. tested circular arches with a constant cross-section and different span-to-height ratios subjected to various load conditions (Bensalem et al, 1998). By disregarding the problem of buckling, steel circular arches with a range of span-to-height ratio between 2 and 8 were investigated using non-linear static *FE* analysis under different load regimes. It was also noted that, as long as the level of loading remains that much lower than the serviceability limit, the analysis can be expanded to arches built of other materials. It was shown that the minimum collapse load occurred at the *L:h* ratio of 2 when the arches were subjected to a vertical uniformly distributed load. Also, the collapse load of a semi-circular arch was about half of the collapse load when the *L:h* ratio of the arch was 3. This finding shows the sensitivity of the behavior of the circular arch with a changing *L:h* ratio. The maximum collapse load was found for a *L:h* ratio between 4 and 5. Moreover, because of the low level of loading in their tests, which could not exceed the linearity state, they compared their results with those obtained from tests on masonry or concrete arches. The comparison demonstrated a fairly good correlation for the range of span-to-height ratio which has the highest collapse load. In spite of the remarkable findings for the optimal range of span-to-height ratio with the criterion of maximum collapse load, only the arches of circular shapes were analyzed.

There are many investigations through the typical range of *L:h* ratios of arches. However, there is no valid reference as to the *L:h* ratio that should be considered the limit for the shallowness of arches at which the arch action is assured. Although, there exists a concrete arch bridge with the highest *L:h* ratio equal to 11.2 (Fonseca and Mato, 2005), masonry arch bridges were frequently built in past centuries at *L:h* ratios of between 3 and 8 (Salonga and Gauvreau, 2010). Increase of the arch shallowness has a transforming effect on the behavior of arch to beam behavior. The commonly used range of *L:h* ratios for arch bridges was suggested between 4.5 and 6, in which there is no need to consider the rib shortening effect (Gaylord and Gaylord, 1990 and Merritt, 1976). The practical limits of the *L:h* ratio of masonry arch structures under permanent loads are an essential part of the design. This limit can be presumed as the effective behavior of arch structures, beyond which the arch behavior is reduced due to flexural response. This is because of the linear relationship of arch shallowness to axial deflections and bending moments.

Despite the wealth of literature on the topic of arch structures, to the best of the author's knowledge, a comprehensive assessment of known shape arches has not been done before. In other words, there is no pervasive study of the effects of arch forms and span-to-height ratios on structural action. Understanding the effects of structural form on the resulting effects of structural actions will assist designers in building structures that are more durable and efficient in material usage. A comprehensive assessment of the behavior of arches, highlighting the effects of arch forms and *L:h* ratio on structural action, is carried out in this paper using a finite element analysis structural software (*GSA*). Therefore, the optimal arch shape for different ratios of *UDL:SW* is investigated. Also, the optimal range of *L:h* ratio in which the combined stresses reaches its minimum and the limit of arch shallowness are studied.

2. Exploring the effect of form and *L:h* ratio of commonly used form of arches

Here, the effects of the arch form, as well as *L:h* ratio on bending moments, displacements, and stresses of the structure are being studied.

2.1. Common shape arches

It is possible, using computational or physical form-finding experiments, to show that an optimum shape of an arch depends on the predominant loading applied to it, see Figure. 1. Thus, provided the arch has a constant cross-section, a circular arch represents an optimum form for the case of a constant radial load, parabolic arch- for a weightless structure under *UDL*, and catenary arch- for the case of self-weight *SW* only (Proske and Pieter, 2009).

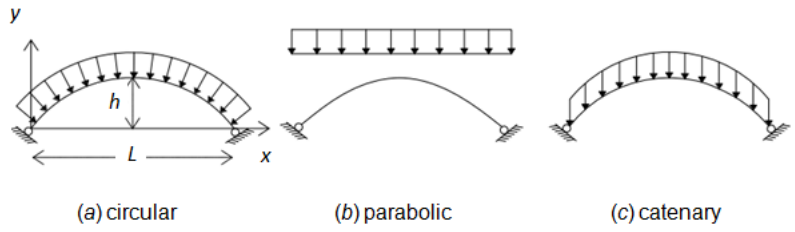

Figure 1. Optimal arch shape according to different loading pattern (Proske and Pieter, 2009)

2.2. Optimality criterion

There are many parameters that need to be considered when designing a structure. The efficient structural form for a masonry rib arch is one that shows the lowest bending moment and combined stress due to bending and thrust. The minimum combined stress is used as a criterion of evaluating the structural performance of arch forms in this paper.

3. Case Studies

The arches to be analysed are of a constant rectangular cross-section of uniform lineal density, supporting a superstructure of uniform density per unit span. Their span is 10 m in each case. Concrete is considered as the construction material, with the elastic modulus of 27 GPa, density 2400 kg/m^3 and the cross-section area of 300 mm by 1000 mm.

To analyze different shapes of arches multiple load cases are applied to them that produce different ratios of *UDL*:*SW*, as listed below:

- *A1*: *UDL* of 20 kN/m applied across full span of the arch plus *SW*.
- *A2*: *UDL* of 20 kN/m applied across the full span of the arch, SW, plus an additional *UDL* of 20 kN/m applied to half the span.
- *A3*: *SW* only.
- *A4*: *UDL* of 20 kN/m applied across full span of the arch only.

It should be noted that load case *A1* presents *UDL:SW* > 1 for the defined arch specifications which gives *SW* equal to 7.2 kN/m.
Decreasing the height of the arches increases axial deformations and bending moments in them. By raising the external load applied to shallow arches, the in-plane structural actions such as axial forces and bending moments develop into nonlinear mode. This means that, the in-plane behavior of arches can turn into either an asymmetric bifurcation or a symmetric snap-through buckling modes (Bradford et al, 2007). To obtain the critical value of the intensity of the loading (w_{cr}) that causes this buckling, Timoshenko stability equation of arches can be used (Timoshenko and Gere, 1961), as $w_{cr} = \gamma_2 \left(EI/L^3\right)$. In which, *E*, *I* and *L* are: the modulus of elasticity, second moment of area, and the span of the arch, respectively. The numerical factor γ_2 depends on the *L:h* ratio. The results of the w_{cr} for the masonry parabolic arch under load case *A4* are presented in Table 1.

Table 1. The critical values of the intensity of the load for the parabolic arch under *UDL* only (Timoshenko and Gere, 1961)

L:h	γ_2	w_{cr}(kN/m)	w_{cr}:*UDL*
2	38.4	2330	117
2.5	43.9	2670	133
3.33	46.5	2820	141
5	45.4	2760	138
10	28.5	1730	86

The *UDL* of 20 kN/m that is the applied load across the full span of the arch can be compared with w_{cr} for parabolic arch from Table 1. As shown above, even for *L:h* ratio of 10 the critical load is 86 times greater than the applied *UDL*. As a result, the studied parabolic arch is stable under 20 kN/m *UDL* only (load case *A4*) applied across the full span of the arch for the range of *L:h* ratios considered. The same can be concluded for other arch forms in this study for *UDL* only load case. This analysis can be conducted when the general combination of *UDL* and *SW* (load case *A1*) are applied to the arches in the case of shallow arch. Since for shallow arches *UDL* and *SW* are adopted, the imposed load can be presumed as the sum of *UDL*+*SW*, which is equal to 27.2 kN/m in this study. Therefore, for flat arches, the loading is still significantly smaller than critical load to buckle. It is concluded that arches are stable for the range of *L:h* ratio between 2 and 8 in this study.
The geometries of parabolic, catenary and circular arches with *L:h* ratios of 2, 3, 5 and 7 are shown in Figure. 2. As shown, the geometrical differences of each form are becoming almost indistinguishable above the *L:h* ratio of 7. The maximum percentage difference between the *y*-coordinate of catenary and parabolic arches of the same span is 14% when *L:h*=2; it reduces to 2% for *L:h* ratio equal to 7.

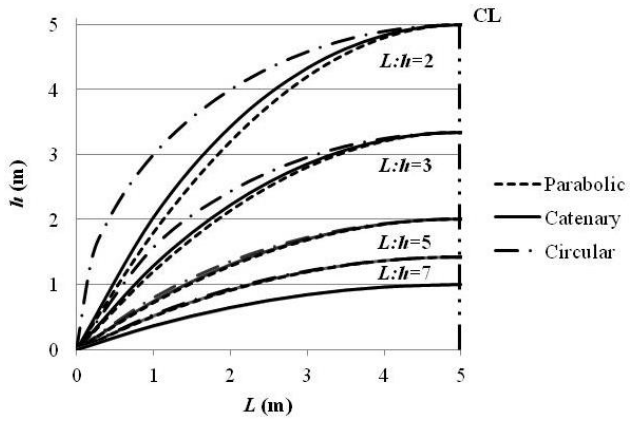

Figure 2. Geometric differences between arches for *L:h* ratios of 2, 3, 5 and 7

4. *FE* analysis results and discussion

To analyze the three most common forms of arches, the computational finite element method provided by the *GSA* software was used. This computational method is based on the Approximate Minimum Degree algorithm for the static analysis of two and three-dimensional structures. For linear analysis, the stiffness matrix method is used in *GSA*. The static analysis of two-pin arches gives the displacement '*u*' as a solution of the linear system of $\{u\} = [K]^{-1}\{f\}$, in which [*K*] is the stiffness matrix for a straight element, and {*f*} is the load or force vector derived from applied load. There to find the forces, Timoshenko beam theory is used and the bending moment in specific direction is based on the stress in that direction. Timoshenko beam theory (Timoshenko, 1986) is used for the semi-rigid analysis of linearly elastic structure based on the second theorem of Castigliano. Using the Castigliano's theorem, the horizontal deflection of an arch, (here analyzed as curved bar) is equal to the derivative of strain energy with respect to the horizontal reaction at a pin. As pin-ended arches are assumed to have no horizontal deflections, the derivative of strain energy with respect to the horizontal reaction force would be zero at the supports. In Castigliano theorem, it is possible to consider strain energy due to bending, shear, thrust and coupling of bending and thrust. But, the coupling of bending and thrust term is not considered when using Timoshenko beam theory in *GSA*.

The curved structures were modelled by a series of straight elements. In order to find an adequate number of elements to model the arch curves, a sensitivity analysis was carried out using variation of bending moments in an arch subjected to load case *A1*, as a function of the number of elements used. It showed 80 elements to be adequate to represent a given arch shape.

Variations of maximum sagging and hogging bending moments with *L:h* ratios and their location for load cases *A1* are presented in Tables 2 and 3 respectively. The ratio of *UDL:SW* for each arch and *L:h* ratio is also given in Table 2. Concerning load case *A1*, due to the symmetry of the geometry and loading, the locations of maximum bending moments and maximum combined stresses are presented for half of the span in the relevant tables.

Table 1. Maximum sagging bending moments (kNm), their locations along the span (m) and *UDL:SW* ratios for the parabolic, catenary, and circular arches; load case *A1*

L:h	Maximum sagging bending moment, (location), *UDL:SW*		
	Parabolic	Catenary	Circular
2	3.55, (1.3), 1.88	8.96, (5), 1.86	50.24, (5), 1.77
3	2.11, (1.4), 2.23	4.97, (5), 2.22	21.44, (5), 2.18
4	1.57, (1.56), 2.42	3.52, (5), 2.41	12.27, (5), 2.40
5	1.44, (1.8), 2.53	3.03, (5), 2.53	8.45, (5), 2.52
6	1.60, (2.4), 2.60	3.03, (5), 2.59	6.71, (5), 2.59
7	2.08, (3.8), 2.64	3.32, (5), 2.64	5.98, (5), 2.64
8	2.85, (5), 2.67	3.81, (5), 2.67	5.82, (5), 2.67

In general, for load case *A1* where *UDL:SW* > 1, circular arch presents the minimum *UDL:SW* due to its higher weight than catenary and parabolic arches for the same *L:h* ratio and *UDL*, while parabolic arch shows the maximum *UDL:SW* amongst the three known shapes. Comparing maximum bending moments of three arches in Table 2, the one with the lower weight (higher *UDL:SW*) behaves in a more efficient way. The maximum sagging bending moment for parabolic and catenary arches is decreasing with the increase of *L:h* from 2 to 5. The trend of decreasing bending moments is then reversed above this ratio. In the case of circular arch, the minimum sagging bending moment is observed at *L:h*=8. Above *L:h* ratio of 8, the differences of sagging bending moments of different arch shapes start getting smaller. Also, the location of maximum sagging bending moment for all three shapes of arches are similar at this *L:h* ratio.

Table 3. Maximum hogging bending moments (kNm) and their locations along the span (m) for the parabolic, catenary, and circular arches; load case *A1*

L:h	Maximum hogging bending moment, (location)		
	Parabolic	Catenary	Circular
2	3.52, (5)	8.11, (1.25)	60.96, (0.37)
3	1.31, (5)	4.64, (1.25)	26.01, (0.87)
4	0.22, (5)	2.78, (1.25)	14.20, (1.12)
5	NA	1.64, (1.12)	8.71, (1.12)
6	NA	0.88, (0.87)	5.67, (0.87)
7	NA	0.37, (0.62)	3.74, (0.87)
8	NA	0.07, (0.12)	2.40, (0.75)

- NA indicates that there is no hogging bending moment.

According to the results of Table 2 (Load case *A1*), the maximum sagging bending moments in catenary and circular arches are observed at the crown of the arch. While, the location of maximum sagging bending moment of parabolic form is near the supports for *L:h* ratio of 2. Then this location moves from near the supports to the crown with increasing *L:h* ratio from 2 to 8. The hogging bending moment of three arches are decreasing with the increase of *L:h* ratio (Table 3). Also, the location of maximum hogging bending moment of parabolic arch is at the crown, but this location is far from crown in the case of catenary and circular shapes. The sagging bending moments in parabolic and catenary arches are dominant compared to the hogging ones, for any *L:h* ratios, while, in circular arches, hogging bending moments are higher than the sagging ones when *L:h*<6. This shows that the tensile forces in circular arches are higher than compressive ones having arch pure behaviour, where the arch could carry 90% of the applied load in compression (*L:h*≤5). The differences in the bending moments for the three arches are demonstrated in Figure. 3.
It is interesting to compare the bending moments of circular arch with the other two forms, for high *L:h* ratio. The geometrical differences of the three shapes of arches are indistinguishable for *L:h* above 7, see Figure. 2, but there is still a difference in the results of bending moments, see Tables 2 and 3.

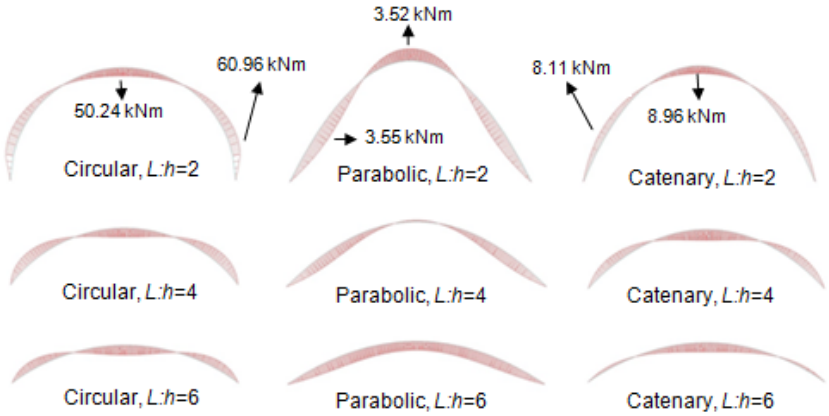

Figure 3. *FE*: Bending moments of three arches for *L:h* ratios of 2, 4 and 6; load case *A1*

To have a general conclusion on the bending moment performance of three arches, the maximum sagging and hogging bending moments and their locations within the arches are shown in Tables 4 and 5 respectively for load case A2 (patch loading).

Table 4. Maximum sagging bending moments (kNm) and their locations along the span (m) for the parabolic, catenary, and circular arches; load case *A2*

L:h	Maximum sagging bending moment, (location)		
	Parabolic	Catenary	Circular
2	33.12, (7.81)	32.81, (6.69)	79.33, (5.94)
3	32.59, (7.69)	30.80, (7.06)	43.80, (6.28)
4	32.63, (7.69)	30.98, (7.31)	34.70, (6.56)
5	32.89, (7.69)	31.61, (7.31)	32.30, (6.81)
6	33.33, (7.56)	32.36, (7.44)	32.02, (6.96)
7	33.91, (7.56)	33.17, (7.44)	32.53, (7.06)
8	34.61, (7.56)	34.03, (7.44)	33.37, (7.19)

Table 5. Maximum hogging bending moments (kNm) and their locations along the span (m) for the parabolic, catenary, and circular arches; load case *A2*

L:h	Maximum hogging bending moment		
	Parabolic	Catenary	Circular
2	30.15, (2.75)	38.27, (1.75)	95.30, (0.75)
3	30.13, (2.63)	34.73, (2)	56.37, (1.25)
4	29.97, (2.63)	32.85, (2.13)	43.55, (1.5)
5	29.67, (2. 5)	31.63, (2.25)	37.84, (1.88)
6	29.23, (2. 5)	30.64, (2.25)	34.66, (2)
7	28.66, (2. 5)	29.73, (2.38)	32.59, (2.13)
8	27.98, (2.38)	28.85, (2.38)	30.99, (2.25)

Comparing Tables 4 and 5, for load case *A2*, sagging bending moments in parabolic arches are higher than hogging ones for any *L:h* ratio. However, catenary and circular arches present higher hogging bending moments than sagging ones when *L:h* ratio is smaller than 6 and 8 respectively. Hence due to the lack of tensile strength of masonry material, parabolic arch is preferred in design once the arch is constructed using concrete and *UDL>SW*. While, circular is an undesirable arch form concerning the results of maximum bending moments.

In theory, catenary and parabolic arches assume to be moment-less for *SW* only, and *UDL* only, respectively (Megson, 2006 and Millais, 2005). This is true only when ignoring the arch shortening/deformation in statical calculations. The *FE* modelling, based on a deformable arch model, produced results that show the catenary arch developing some moments, which increase with the *L:h* ratio (Figure. 4). Similar observation can be made with respect to load case *A4* and the parabolic arch, (Figure. 5) which also develops small bending moments. In both of these cases if a non-deformable model was used, the bending moments would have been equal to zero. In general, catenary and parabolic arch cannot assume as momentless form when *L:h* exceeds 5 for *SW* only and *UDL* only load cases. Since, the arch carries the applied load developing bending moment as well as axial forces when *L:h* > 5, this ratio can be considered as the limit of the arch shallowness.

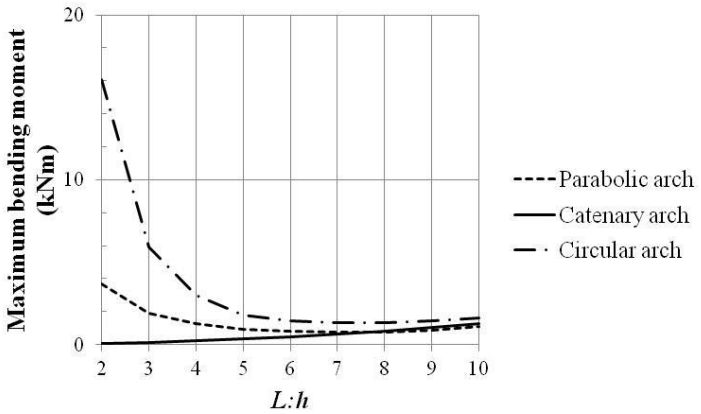

Figure 4. *FE*: The absolute value of maximum bending moment against *L:h* ratio; load case *A3*(SW only)

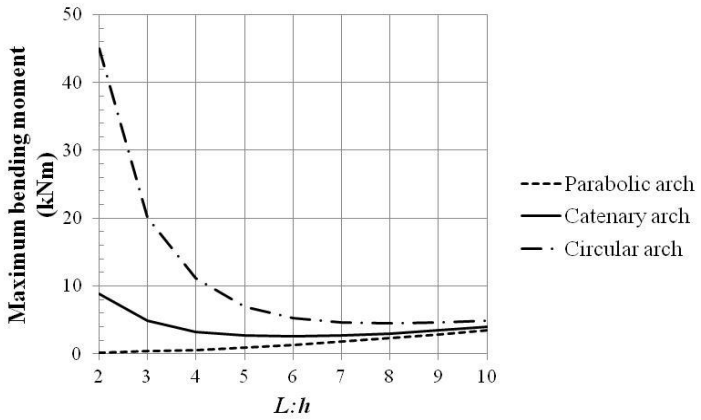

Figure 5. *FE*: The absolute value of maximum bending moment against *L:h* ratio; load case *A4* (UDL only)

For a very high *L:h* ratio, an arch becomes a beam. The *FE* results showed that the maximum bending moments in the three arches at *L:h*=8 were found almost less than 10% of the maximum bending moment of the equivalent beam (when *L:h* ratio was taken as 300). This applied to all load cases.

As it was stated previously, the *L:h* ratio at which the combined stress due to bending and compressive axial force reaches its minimum is considered as optimal. The results of the maximum combined stress against *L:h* ratio and their location within the arch, for the three types of arches and load cases *A1* and *A2* are shown respectively in Tables 6 and 7. The maximum values of thrust for these load cases are also presented in Table 8. The location of maximum value of thrust for all load cases is at the arch supports.

Table 6. Maximum combined stresses (MPa) and their locations along the span (m) for the parabolic, catenary, and circular arches; load case *A1*

L:h	Maximum combined stress, (location)		
	Parabolic	Catenary	Circular
2	0.69, (1)	0.99, (1)	4.54, (0.5)
3	0.65, (1)	0.82, (1)	2.24, (1)
4	0.69, (1)	0.77, (1)	1.52, (1)
5	0.76, (1)	0.79, (1)	1.25, (1)
6	0.85, (1)	0.88, (4.75)	1.14, (1)
7	0.96, (1.5)	1.01, (4.75)	1.18, (4.75)
8	1.09, (3)	1.15, (4.75)	1.28, (4.75)

Table 7. Maximum combined stresses (MPa) and their locations along the span (m) for the parabolic, catenary, and circular arches; load case *A2*

L:h	Maximum combined stress, (location)		
	Parabolic	Catenary	Circular
2	2.70, (7.75)	3.05, (2)	6.92, (0.5)
3	2.76, (7.75)	2.91, (2)	4.38, (1)
4	2.88, (7.75)	2.90, (2)	3.63, (1.5)
5	3.03, (7.75)	2.95, (2)	3.37, (2)
6	3.20, (7.75)	3.12, (7.25)	3.30, (2)
7	3.38, (7.75)	3.32, (7.25)	3.30, (2)
8	3.57, (7.25)	3.53, (7.25)	3.47, (7.25)

Table 8. Maximum thrust (kN) for the parabolic, catenary, and circular arches; load case *A1*and *A2*

L:h	Load case *A1*			Load case *A2*		
	Parabolic	Catenary	Circular	Parabolic	Catenary	Circular
2	168.8	168	161.2	247	246.5	238.1
3	178.3	177.3	172.3	260.7	260	255.1
4	197	196	192.8	285.2	284.4	281.5
5	220.3	219.3	216.9	315.6	314.8	312.5
6	246.2	245.4	243.4	349.8	348.9	347
7	273.8	273.1	271.4	386.3	385.5	383.8
8	302.5	301.8	300.3	424.5	423.8	422.1

Comparing the results from Tables 2 and 3 with the results in Table 6 for combined stresses, load case *A1*, the values of both maximum bending moment and maximum combined stress do not occur at the same *L:h* ratio for each arch shape.

The results for maximum combined stress for circular arches differ significantly from the results for parabolic and catenary shapes, particularly for *L:h* ratio below 5. The circular arch shows high sensitivity to changes in *L:h* ratio and the maximum combined stress reaches a minimum value at *L:h* ratio between 4 and 6. The minimum combined stresses in parabolic and catenary shapes are observed at *L:h* ratio between 2 and 4 when both *UDL* and *SW* are applied. Here, the parabolic arch shows a lower bending moment and combined stress than catenary and circular arches. Parabolic arches experience a dramatic increase in combined stress for load case *A2* (load case *A1* + patch load). Here, their performance does not differ much from that of the other two types of arches.

Overall, the results show that both the form and the *L:h* ratio strongly influence structural response, and this applies to all load cases.

The arches are made of concrete, a material known to have low tensile strength. Therefore, it is worth examining whether, the maximum combined stresses become tensile. The results are presented in Table 9. Assuming the maximum tensile strength of concrete to be 3 MPa (for concrete of characteristic strength of ~ 30 MPa), the results demonstrate that tensile stresses in all arches are lower than the maximum tensile strength of the material, except in the case of a circular arch under load cases *A1* and *A2* and *L:h* ratio of 2. This has implication for both design and the method of analysis, because we cannot assume the material is behaving elastically at this level of tension. However, these are isolated load cases, which can be dealt with by using a higher *L:h* ratio in design.

Table 9. Combined tensile stresses (MPa) of the parabolic, catenary, and circular arches; all load cases

L:h	Parabolic arch				Catenary arch				Circular arch			
	A1	*A2*	*A3*	*A4*	*A1*	*A2*	*A3*	*A4*	*A1*	*A2*	*A3*	*A4*
2	NA	1.73	0.17	NA	0.36	2.06	NA	0.43	3.59	5.78	0.92	2.67
3	NA	1.60	0.01	NA	NA	1.73	NA	0.08	1.23	3.14	0.25	0.98
4	NA	1.48	NA	NA	NA	1.48	NA	NA	0.38	2.18	0.05	0.33
5	NA	1.36	NA	NA	NA	1.29	NA	NA	0.01	1.67	NA	0.04
6	NA	1.25	NA	NA	NA	1.19	NA	NA	NA	1.33	NA	NA
7	NA	1.14	NA	NA	NA	1.10	NA	NA	NA	1.08	NA	NA
8	NA	1.04	NA	NA	NA	1.01	NA	NA	NA	0.98	NA	NA

- NA indicates that there is no tensile stress.

The resultant maximum displacements for the three types of arches are presented in Figures. 6 and 7, for load cases *A1* and *A2*, respectively. As expected, catenary and parabolic arches display lower resultant displacements when the loading is *SW* only (*A3*), and *UDL* only (*A4*), respectively.

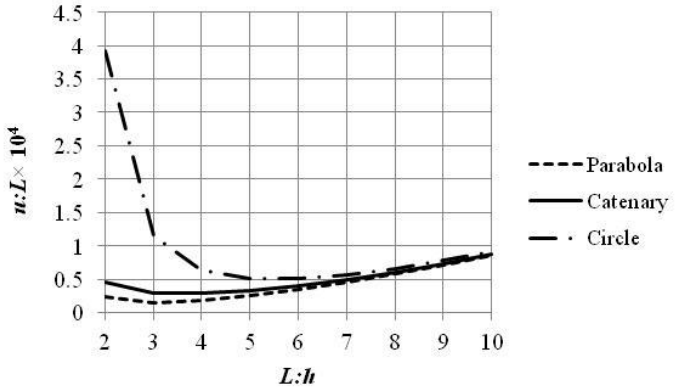

Figure 6. *FE*: Maximum resultant displacements against *L:h* ratio; load case *A1*

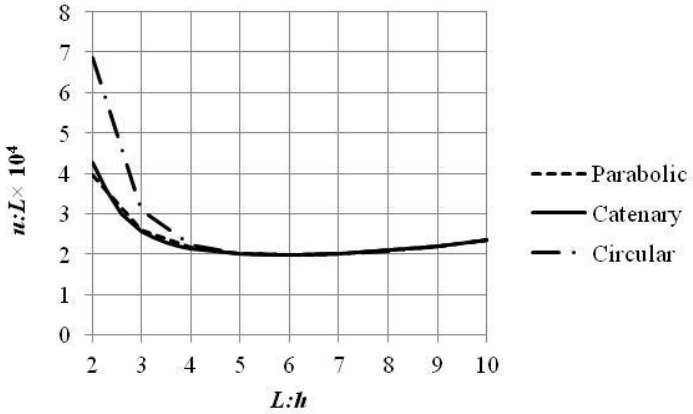

Figure 7. *FE*: Maximum resultant displacements against *L:h* ratio; load case *A2*

It can be seen that the variation of maximum resultant displacement with *L:h* ratio follows a similar trend for load cases *A1* and *A2*. It has been found that the trend for load cases *A3* and *A4* is similar.
The circular form, with *L:h* ratio between 2 and 5, shows the highest magnitude of maximum resultant displacements compared with the other two forms. For parabolic and catenary arches under the load case *A1*, the difference in displacement between the two falls from 50% at *L:h* ratio of 2, to 21% at *L:h* ratio of 5. In general, parabolic arch shows a lower displacement than catenary and circular form when *UDL:SW* > 1. The differences of resultant displacements of parabolic and catenary arches are negligible for load case *A2*.
The deformed shapes of circular, parabolic, and catenary arches for load case *A1* and the *L:h* ratio of 2, 4 ,and 6 are illustrated in Figure. 8.

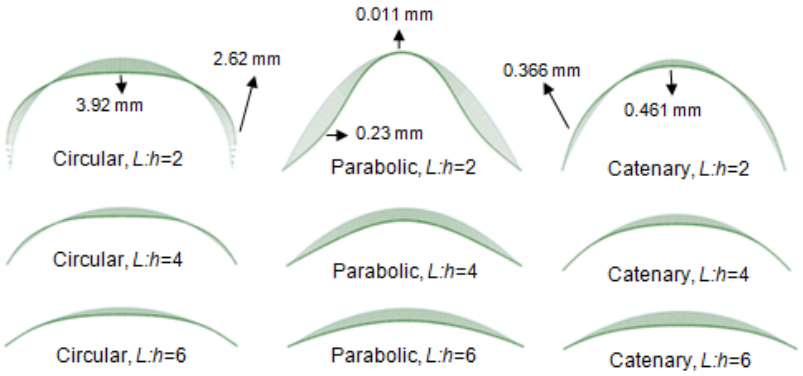

Figure 8. *FE*: Deformed shapes of the circular, parabolic, and catenary arches for *L:h* of 2, 4, and 6; load case *A1*

The catenary and circular arches displaced in the same way, but significantly different from parabolic arch (Figure. 8). This indicates the failure mode of the parabolic arch to be completely different compared to the failure mode of the other two arches. Comparing Figure 3 and 8, the behavior of bending moment is similar to the displaced form for each arch shape.

The parabolic arch displaced similarly for load cases *A1*, *A3*, and *A4*. However, the magnitudes of displacements are different. With regard to the load case *A2* (presence of patch load), the arch displaced much more, and in different shape compared to other load cases. All three types of arches showed similar deformed shapes under this load case. The *L:h* ratio of 4 is the ratio at which the differences in displaced shapes of arches are small but still significant and we have chosen this ratio for a further deformation analysis. The deformed shape of parabolic arch under load case *A2* for *L:h*=4 is shown in Figure. 9.

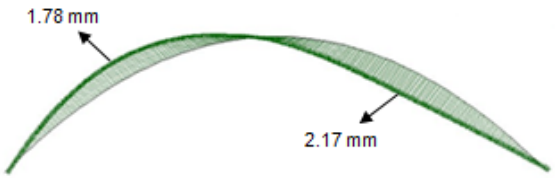

Figure 9. *FE*: Deformed shape of the parabolic arch for *L:h* = 4; load case *A2*

Figure. 10 illustrates the horizontal reaction forces in all three types of arches for load case *A1*. The results show linear dependence on the *L:h* ratio and slight differences in the reactions for the *L:h* ratio below 5. Above this ratio, the horizontal reaction forces are similar in all arches, and yet the maximum bending moments (Tables 2 and 3) and maximum combined stresses (Table 6) show significant differences. Such behavior suggests that very small variations in horizontal reactions have a substantial influence on the behavior of each structure.

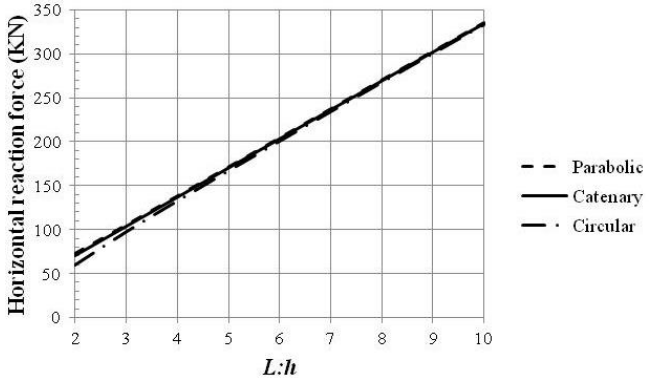

Figure 10. *FE*: The horizontal reaction force against *L:h* ratio; load case *A1*

The whole analysis was carried out for the same arch specifications and *UDL* of 2.6 kN/m and 7.2 kN/m that give respectively *UDL:SW* < 1 and *UDL:SW* = 1. Overall, the parabolic arch is more efficient, exhibiting lower bending, displacements, and combined stresses than the other two arches when *UDL:SW* > 1. The catenary arch is preferable when *UDL:SW* < 1 considering the minimum structural action effect criterion. The differences in the results of structural actions are negligible between the catenary and parabolic arches for *UDL:SW* = 1. Finally, the circular arch demonstrates the least desirable results for any ratios of *UDL:SW*.

5. Arches of steel material

For a general conclusion on the optimal arch form and *L:h* ratio, a hollow steel cross-section with a width of 200 mm, depth of 400 mm, and thickness of 13 mm was also analyzed using the *GSA* software. This cross-section gives a flexural rigidity *EI*, that is the same as a concrete solid cross-section. The elastic modulus and density of the steel material are assumed to be 205 GPa and 7850 kg/m^3 respectively. It should be noted that the weight of concrete arches is 6 times greater than the weight of arches of the steel material with the properties given in this section. This means that the *UDL:SW* ratio of the three forms of arches constructed from steel is 6 times larger than the *UDL:SW* of the three studied shapes of concrete arches for any *L:h* ratio.

As stated previously, the optimal range to the *L:h* ratio is found when the maximum value of the combined stress reaches its minimum. Results to the absolute values of the maximum combined stress against *L:h* ratio under load case *A1* are plotted in Figures 11 and 12 using concrete and steel as the construction material, respectively.

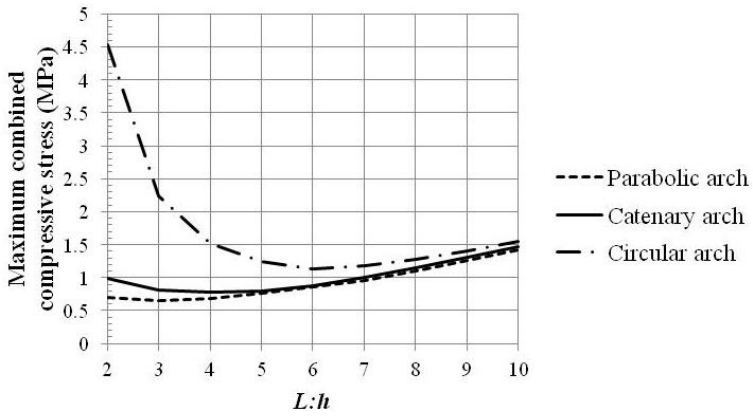

Figure 11. *FE*: The absolute value of the maximum combined stresses against *L:h* ratio using concrete material for load case *A1*

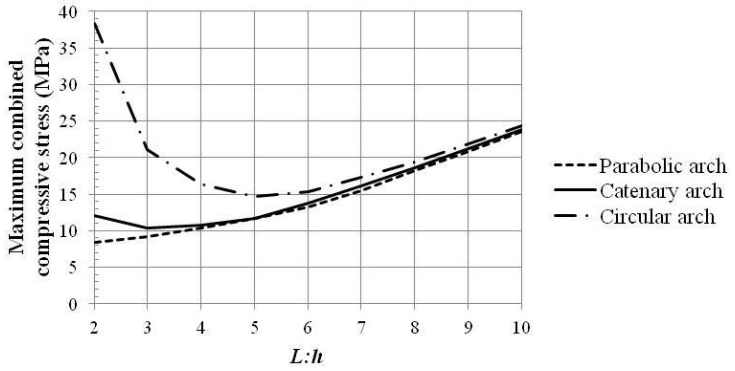

Figure 12. *FE*: The absolute value of the maximum combined stresses against *L:h* ratio using steel material for load case *A1*

The results of the maximum combined stress for the circular arch differ significantly from the results of the parabolic and catenary forms, particularly for *L:h* ratios below 5 for arches of both steel and concrete

material. In general, the maximum combined stress reaches its minimum at *L:h* ratios between 2 and 4 for the parabolic and catenary arches under all load cases. Meanwhile, the optimal *L:h* ratio of the circular shape is between 4 and 6. The behavior of both steel and concrete arches is the same under each load case. The magnitudes of the structural actions obtained from steel arches are different from those assuming arches built of concrete. The arches made of steel shows about 90% higher combined stresses than concrete arches for different *L:h* ratios.

6. Conclusion

A numerical structural analysis of three well-known forms of arches, namely: parabolic, circular, and catenary suggests; both arch shapes and the *L:h* ratio have significant impacts on the resulting effects of structural actions. It was concluded that circular arches are very sensitive to the variation of *L:h* ratio and show large differences in the results of bending moments and combined stresses compared to the two other arch forms. In general, the optimum range of *L:h* ratio for catenary and parabolic arches is between 2 and 4, while for circular arches, it is limited to *L:h* ratio between 4 and 6, when using a minimum combined stresses criterion. These results are adoptable for any *UDL:SW* ratio and for arches made of masonry, concrete, and steel material. But, the combined stress in arches of steel material is more than about 75% higher than the combined stresses for concrete arches. From the structural behaviour results of all three arch shapes, it is concluded that arches are becoming shallow for *L:h*>5. It was seen that maximum combined stress and bending moments of catenary and parabolic forms are increasing when *L:h* ratio increases above 5. Also, the parabolic and catenary arches demonstrated lower structural action effects when respectively *UDL*>*SW* and *SW*>*UDL*. But, both arches behave in the same way in the case of *UDL* = *SW*.

References

Ambrose, J. & Tripeny, P. (2011). Building Structures, 3rd Edition, John Wiley & Sons, Inc., New Jersey, USA

Austin, W.J. & Ross, T.J. (1976). Elastic Buckling of Arches under Symmetrical Loading, Journal of Structural Division ASCE, Vol. 120, 1085-1095

Bensalem, A., Sibbald, A. & Fairfield, C.A. (1998). The use of dynamic characteristics for the optimal design of arches, Computers and Structures, Vol. 68, No. 5, 461-472

Bradford, M.A., Pi, Y.-L., & Tin-Loi, F. (2007). Nonlinear analysis and buckling of elastically supported circular shallow arches, Solids and Structures, Vol. 44, No. 7-8, 2401-2425

Fairfield, C.A. & Ponniah, D.A. (1994). Model tests to determine the effect of fill on buried arches, Proceedings of the Institution of Civil Engineers - Structures and Buildings, Vol. 104, No. 4, 471-482

Fonseca A. & Mato, F. (2005). Infant Henrique Bridge over the River Douro, Structural Engineering International, Vol. 15, No. 2, 85-87

Gaylord E.H. & Gaylord C. N. (1990). Structural Engineering Handbook. McGraw-Hill Publishing Company, New York

Harvey, W.J. & Smith, F.W. (1987). Semicircular arches, Proceedings of the Institution of Civil Engineers, Vol. 85, No. 4, 845- 849

Heyman, J. (1998). Hooke's cubico-parabolical conoid, Notes Rec. Royal Soc. Vol. 52, 39-50

Heyman, J. (1998) Structural Analysis: A Historical Approach. Cambridge: Cambridge University Press

Megson, T. H. G. (2006). Structural and Stress Analysis, 2nd Edition, Elsevier, Oxford, UK

Merritt F. S. (1976). Standard Handbook for Civil Engineers, McGraw-Hill Book Company, New York

Millais, M. (2005). Building Structures: from concepts to design, 2nd Edition, Spon Press, Abingdon, UK

Proske, D. & Pieter, V.G. (2009). Safety of historical stone arch bridges, Springer

Salonga, J. & Gauvreau, P. (2010). Span-to-rise ratios in concrete arches: threshold values for efficient behaviour', ARCH'10 – 6th International Conference on Arch Bridges, 665-673

Timshenko, S.P. (1986). Strength of Materials. 3rd Edition, CBS Publishers, New Delhi

Timoshenko, S.P. & Gere, J.M. (1961). Theory of Elastic Stability, 2nd Edition, McGraw Hill, New York

Tomlow, J., Graefe, R., Otto, F. & Szeemann, H. (1989). Das Modell / The Model / El Modelo. Number 34 in Mitteilungen des Instituts fr Leichte Flchentragwerke (IL), Institut für Leichte Flächentragwerke, Stuttgart